The correlation between superparamagnetic blocking temperatures and peak temperatures obtained from ac magnetization measurements

2008 J. Phys.: Condens. Matter 20 345209

(http://iopscience.iop.org/0953-8984/20/34/345209)

IOP Publishing Journal of Physics: Condensed Matter
J. Phys.: Condens. Matter **20** (2008) 345209 (6pp) doi:10.1088/0953-8984/20/34/345209

The correlation between superparamagnetic blocking temperatures and peak temperatures obtained from ac magnetization measurements

Daniel Esmarch Madsen[1], **Mikkel Fougt Hansen**[2] and **Steen Mørup**[1]

[1] Department of Physics, Technical University of Denmark, DTU Physics, Building 307, DK-2800 Kongens Lyngby, Denmark
[2] Department of Micro- and Nanotechnology, Technical University of Denmark, DTU Nanotech, Building 345 East, DK-2800 Kongens Lyngby, Denmark

E-mail: demadsen@fysik.dtu.dk

Received 25 March 2008, in final form 16 July 2008
Published 1 August 2008
Online at stacks.iop.org/JPhysCM/20/345209

Abstract
We study the correlation between the superparamagnetic blocking temperature T_B and the peak positions T_p observed in ac magnetization measurements for nanoparticles of different classes of magnetic materials. In general, $T_p = \alpha + \beta T_B$. The parameters α and β are different for the in-phase (χ') and out-of-phase (χ'') components and depend on the width σ_V of the log-normal volume distribution and the class of magnetic material (ferromagnetic/antiferromagnetic). Consequently, knowledge of both α and β is required if the anisotropy energy barrier KV and the attempt time τ_0 are to be reliably obtained from an analysis based solely on the peak positions.

1. Introduction

Magnetic nanoparticles have been a topic of intense research due to their many novel properties [1–6]. However, when studying these new phenomena, attention should be paid to the fact that the traditional ways of analysing and interpreting experimental data may no longer be adequate when dealing with effects induced as a consequence of the finite size. This is particularly important in studies of antiferromagnetic nanoparticles [6]. For example, due to the small magnetic moment in antiferromagnetic nanoparticles, the Zeeman energy is often comparable to the anisotropy energy, which consequently must be considered when analysing, e.g., magnetization data [7]. Moreover, since most samples are not monodisperse, it is important to consider the consequences of the size distribution. Silva *et al* [8] recently discussed the effect of a magnetic moment distribution on the interpretation of magnetization data for antiferromagnetic nanoparticles. Another important aspect is the different size dependence of the magnetic moment for ferromagnetic and antiferromagnetic nanoparticles. In antiferromagnetic nanoparticles at low magnetic fields, the magnetization is due to the presence of an uncompensated moment, which is assumed to have a median size given by

$$\mu_u = \mu_{at} n_u \approx \mu_{at} N^p, \tag{1}$$

where n_u is the number of uncompensated magnetic atoms, N is the total number of magnetic atoms, μ_{at} the magnetic moment per atom, and p is a parameter ranging from $1/3$ to $2/3$ [9–11], which depends on how the uncompensated spins are distributed in the particle. If the nanoparticles have random occupancy of all lattice sites, $p \simeq 1/2$. If the interior of the particles is assumed defect-free, but there is a random occupancy of surface sites, the number of uncompensated spins should be proportional to the square root of the number of surface sites, i.e. $p \simeq 1/3$. In the case of cubic particles consisting of either an even or an odd number of planes with parallel spins, but with alternating magnetization directions, $p \simeq 2/3$. In poorly crystalline antiferromagnetic particles such as ferritin and ferrihydrite it has been found that $p \simeq 1/2$

whereas $p \simeq 1/3$ has been obtained in some samples of NiO nanoparticles [6]. In a ferromagnet, $p = 1$.

In this work we study the relationship between the peak temperature T_p obtained from ac magnetization measurements and the superparamagnetic blocking temperature T_B for several values of p (1/3, 1/2, 2/3, and 1). Although the peak position of the in-phase component (χ') of the ac susceptibility has previously been discussed for some of the above cases [12], to our knowledge this is the first time that the relationship between T_B and the peak positions of both the in-phase (χ') and out-of-phase (χ'') component is systematically studied.

2. Theory

Superparamagnetic relaxation takes place when the thermal energy $k_B T$ becomes sufficiently large in relation to the anisotropy energy barrier separating the easy directions of magnetization. In that case it becomes possible for the magnetization to surmount this barrier. It is often assumed that the magnetic anisotropy is uniaxial with an anisotropy energy given by

$$E_a = KV \sin^2\theta, \tag{2}$$

where K is the anisotropy constant, V is the volume of the particle, and θ is the angle between the magnetization direction and the easy axis of magnetization. Equation (2) represents two energy minima separated by an energy barrier of height KV. For non-interacting particles the average time between magnetization reversals is usually assumed to be given by the Arrhenius-like Néel–Brown expression [13, 14]

$$\tau = \tau_0 \exp\left(\frac{KV}{k_B T}\right), \tag{3}$$

where $\tau_0 \sim 10^{-9}$–10^{-13} s and depends only weakly on temperature. Experimental data are usually obtained as the result of measuring a signal on a timescale τ_m, characteristic of the experimental method. If $\tau \ll \tau_m$, the observed magnetization will be the thermal equilibrium value. On the other hand, if $\tau \gg \tau_m$, the observed magnetization will appear static. The temperature at which $\tau_m = \tau$ is denoted the blocking temperature T_B. Since for a single particle

$$KV = -\ln\left(\frac{\tau_0}{\tau_m}\right) k_B T_B, \tag{4}$$

T_B is directly related to the size of the energy barrier. In the presence of a distribution of volumes, the blocking temperature refers to a suitable parameter of this distribution, either the median volume V_m or the average volume $\langle V\rangle$. In this work, we relate the blocking temperature to the median volume V_m of a volume-weighted volume distribution (i.e., particles with $V < V_m$ constitute half the total volume). Note, that in the case of ac susceptibility, τ_m is related to the angular frequency $\omega = 2\pi f$ of the applied field rather than its frequency f, that is, $\tau_m = 1/\omega$ [15, 16].

From an experimental point of view, one is often interested in determining the blocking temperature in order to obtain knowledge about the anisotropy energy barrier and τ_0 of a given sample. In magnetization measurements (dc in zero-field-cooled (ZFC) data, or ac in χ' and χ'' data) a peak in the signal is observed at a temperature T_p, which is often interpreted as the blocking temperature. However, as a number of authors (e.g., [12, 17, 18]) have discussed, the observed peak temperature does not necessarily correspond to the blocking temperature if a distribution of volumes is present. In general, the relationship between the two may be expressed through a parameter β, such that $T_p = \beta T_B$. Gittleman *et al* [12] examined the peak positions of the in-phase component of the ac susceptibility (χ') and found β for a number of simple volume distributions. Jiang and Mørup [17] considered ZFC data using a log-normal distribution of volumes and examined the dependence of β on the width σ_V of the distribution for $p = 1$ and $1/3$. They also found that the value of β is different for ferromagnetic and antiferromagnetic systems.

3. Simulation procedure

In the following, we derive the expressions used to calculate χ' and χ''. Consider a sample subjected to a time-varying magnetic field

$$h(t) = h_0 \cos(\omega t). \tag{5}$$

The resulting magnetization of the sample is

$$M(t) = \chi_{ac}(\omega, T) h(t), \tag{6}$$

where the susceptibility can be written as

$$\chi_{ac}(\omega, T) = \chi'(\omega, T) + i\chi''(\omega, T). \tag{7}$$

χ' and χ'' are the in-phase and out-of-phase components, respectively. These may be found using the model by Gittleman *et al* [12] where the susceptibility in the time domain is expressed as

$$\chi_{ac}(t, T) = \chi_0 + (\chi_\infty - \chi_0)(1 - e^{-t/\tau}). \tag{8}$$

Here, χ_0 and χ_∞ are the susceptibility of the blocked and unblocked (superparamagnetic) particles, respectively. A Fourier transformation of equation (8) yields

$$\chi_{ac}(\omega, T) = \frac{\chi_\infty + i\omega\tau\chi_0}{1 + i\omega\tau}, \tag{9}$$

and insertion of the following expressions for χ_0 and χ_∞ [12]

$$\chi_0 = \frac{\mu_0 M^2(V)}{3K} \tag{10}$$

$$\chi_\infty = \frac{\mu_0 M^2(V) V}{3k_B T} \tag{11}$$

gives

$$\chi_{ac}(\omega, T) = \frac{\mu_0 M^2(V)}{1 + i\omega\tau}\left[\frac{V}{3k_B T} + \frac{i\omega\tau}{3K}\right], \tag{12}$$

which leads to

$$\chi'(\omega, T) = \frac{\mu_0 M^2(V)}{3K}\left(\frac{KV}{k_B T}\frac{1}{1 + (\omega\tau)^2} + \frac{(\omega\tau)^2}{1 + (\omega\tau)^2}\right) \tag{13}$$

$$\chi''(\omega, T) = \frac{\mu_0 M^2(V)}{3K}\left(\frac{\omega\tau}{1+(\omega\tau)^2} - \frac{KV}{k_B T}\frac{\omega\tau}{1+(\omega\tau)^2}\right). \tag{14}$$

Note, that τ also depends on the temperature as given by (3). In the above expressions we have written the magnetization as $M(V)$ to emphasize the volume dependence. It should be noticed that because of the randomness of the occupation of the lattice sites, particles with identical volumes can have different magnetic moments. As shown in the appendix, this can be taken into account by replacing $M^2(V)$ by the second order moment of the distribution of magnetization, μ_u/V, for particles with volume V. Using equation (1), one finds

$$M(V) = \frac{\mu_u}{V} = \mu_{at} c^p V^{p-1}. \tag{15}$$

This is different from ferromagnetic particles where the magnetization is independent of volume. The constant c appearing in this expression is found using that the volume and the number of atoms are related as $N = [zN_A\rho/M_{mol}]V \equiv cV$. Here, ρ is the density of the material, M_{mol} is the molar mass, z is the number of magnetic atoms per formula unit, and N_A is Avogadro's number.

We now proceed by considering a sample with a distribution of volumes. Defining $y = V/V_m$, we get

$$\frac{M(V)}{M_m} = \frac{cV^{p-1}}{cV_m^{p-1}} = y^{p-1}, \tag{16}$$

where M_m is the magnetization of a particle with median volume V_m. We now write the expressions for χ' and χ'' as

$$\chi'(\omega, T) = \frac{\mu_0 M_m^2}{3K}\int_0^\infty \left(\frac{KV_m}{k_B T}\frac{y}{1+(\omega\tau)^2} + \frac{(\omega\tau)^2}{1+(\omega\tau)^2}\right) y^{2p-2} p_V(y)\,dy \tag{17}$$

$$\chi''(\omega, T) = \frac{\mu_0 M_m^2}{3K}\int_0^\infty \left(\frac{\omega\tau}{1+(\omega\tau)^2} - \frac{KV_m}{k_B T}\frac{y\omega\tau}{1+(\omega\tau)^2}\right) y^{2p-2} p_V(y)\,dy, \tag{18}$$

where $p_V(y)\,dy$ is the volume-weighted volume distribution (i.e., the volume fraction of the sample with volume between V and $V + dV$ is $p_V(V/V_m)\,d(V/V_m)$). For the simulations we use the log-normal distribution

$$p_V(y, \sigma_V)\,dy = \frac{1}{\sqrt{2\pi}\sigma_V y}\exp\left(-\frac{\ln^2 y}{2\sigma_V^2}\right) dy, \tag{19}$$

which is commonly encountered in the literature. In the following simulations, V_m enters as a parameter. However, we report for convenience the particle sizes in terms of the diameter d_m of a spherical particle having volume V_m.

4. Results and analysis

The ac susceptibility at different frequencies f as a function of temperature was calculated for $K = 5 \times 10^4$ J m^{-3} and different values of p, σ_V, τ_0 and d_m. For the calculations (with χ' and χ'' in arbitrary units) the parameters c and μ_{at}, can be randomly chosen as they only affect the total scaling through M_m, but not the positions of the peaks. Figure 1 shows examples of the resulting data for selected combinations of p, σ_V, f, and τ_0.

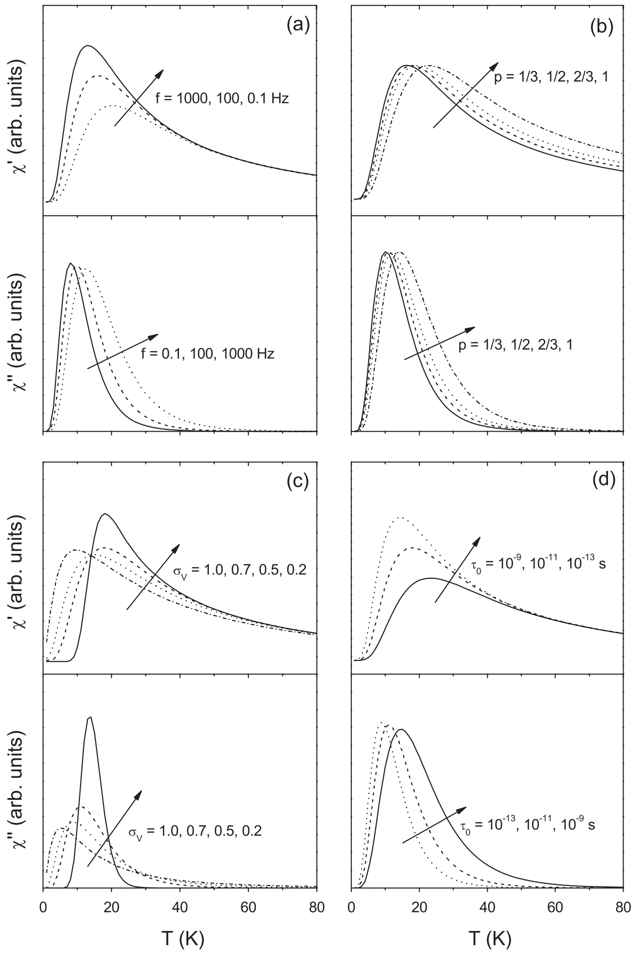

Figure 1. χ' and χ'' as a function of temperature for various values of (a) f, (b) p, (c) σ_V and (d) τ_0. Parameters that were not varied were fixed to $f = 100$ Hz, $\sigma_V = 0.5$, $p = 1/2$, $\tau_0 = 10^{-11}$ s, and $d_m = 5.2$ nm. The curves in (b) were normalized by the peak temperature value.

For each of these datasets the peak positions, designated T'_p and T''_p, for the in-phase and out-of-phase components, respectively, were determined and compared to the value of T_B calculated from equation (4). For each set of the parameters p, σ_V, and τ_0 we obtained a range of (T_p, T_B) values by varying f. Figure 2 shows selected results.

From figure 2 one may notice that T'_p and T''_p, respectively, are approximately linearly related to T_B. This was the case for all combinations of the parameters. Consequently, we have fitted the observed peak temperatures to the expressions

$$T'_p = \alpha' + \beta' T_B \tag{20}$$

$$T''_p = \alpha'' + \beta'' T_B \tag{21}$$

in order to obtain the parameters α and β. Figures 3 and 4 show the results. In all cases excellent fits were obtained. However,

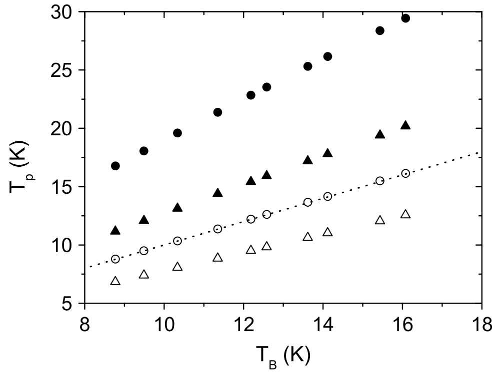

Figure 2. The peak positions T_p' (full symbols) and T_p'' (open symbols) as a function of T_B for selected datasets (triangles: $p = 1/2, \sigma_V = 0.5$, circles: $p = 1, \sigma_V = 1.0$). $\tau_0 = 10^{-11}$ s and $d_m = 5.2$ nm were used in the simulations. The dotted line corresponds to $T_p = T_B$.

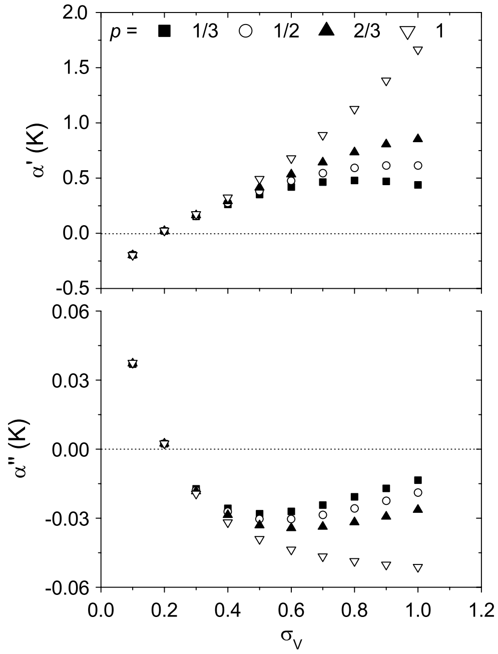

Figure 3. α' and α'' as a function of σ_V. The values $\tau_0 = 10^{-11}$ s and $d_m = 5.2$ nm were used in the calculations.

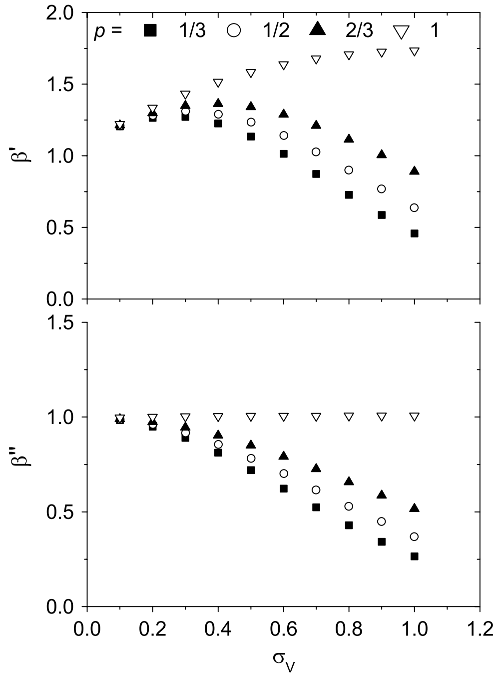

Figure 4. β' and β'' as a function of σ_V. The values $\tau_0 = 10^{-11}$ s and $d_m = 5.2$ nm were used in the calculations.

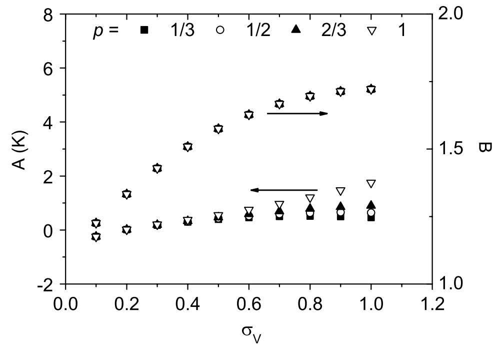

Figure 5. The parameters A and B as a function of σ_V. The values $\tau_0 = 10^{-11}$ s and $d_m = 5.2$ nm were used in the calculations.

it was necessary to have $\alpha \neq 0$. We obtained similar results for other values of τ_0 and d_m.

It can be seen from figure 3 that α' increases with increasing σ_V and that α' varies considerably with p. For $\sigma_V > 0.8$ and $p = 1/3$, α' is found to decrease slightly. Although α'' exhibits some dependence on p, its magnitude remains almost negligible compared to the peak temperatures.

From figure 4 it is seen that β' increases with increasing σ_V in the entire range only for $p = 1$, whereas for $p < 1$, β' first increases slightly and then decreases for $\sigma_V > 0.3$. This is in agreement with the calculations by Jiang and Mørup [17]. β'' remains close to 1 for $p = 1$, whereas for $p < 1$, it decreases with increasing σ_V.

It is interesting to consider the dependence of T_p' on T_p'', which we write as $T_p' = A + BT_p''$. According to (20) and (21), $A = \alpha' - (\beta'/\beta'')\alpha''$ and $B = \beta'/\beta''$. Figure 5 shows the values of A and B calculated from the parameters shown in figures 3 and 4. It is remarkable that the values of B all fall on the same line for all p values. The values of A, however, show some variation. Figure 6 shows B for other values of τ_0 and d_m. As one may notice, slightly different curves are found for other values of τ_0. However, no differences were observed if d_m was changed. A (not shown) showed some dependence on all parameters.

5. Discussion

The values of τ_0 and KV_m can be determined from an analysis of $\ln(\omega)$ versus $1/T_B$. As equation (3) can be rewritten

$$\ln(\omega) = \ln(1/\tau_0) - \frac{KV_m}{k_B}\frac{1}{T_B}, \qquad (22)$$

this should give a straight line with slope $-KV_m/k_B$ and intersect $\ln(1/\tau_0)$ at $1/T_B = 0$. If, as it is common, T_p is

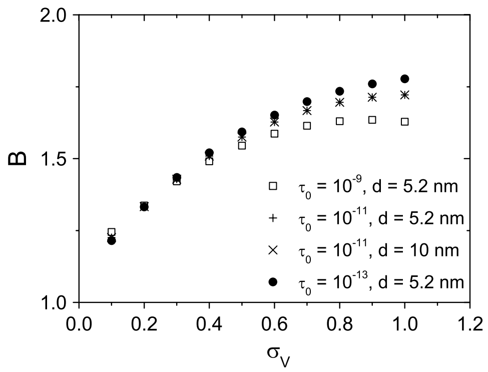

Figure 6. The parameter B for $p = 1/2$ and various values of τ_0 and d_m.

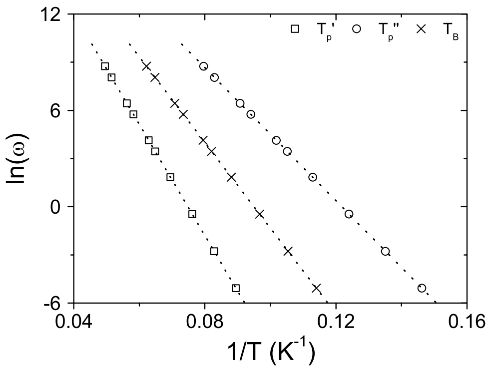

Figure 7. $\ln(\omega)$ as a function of $1/T_p$, with T_p obtained from simulated χ' (□) and χ'' (○) data (with $p = 1/2$, $\sigma_V = 0.5$, and $\tau_0 = 10^{-11}$ s), respectively. We also show the fits to equation (22) (lines), and, for comparison, $\ln(\omega)$ as a function of $1/T_B$ (×).

taken as T_B, erroneous values of τ_0 and KV_m will be obtained. Figure 7 illustrates this problem. We plot $\ln(\omega)$ as a function of $1/T_p$ for a selected dataset, in this case with $p = 1/2$, $\sigma_V = 0.5$, and $\tau_0 = 10^{-11}$ s. The corresponding plot with the real values of $1/T_B$ is shown for comparison. The difference is quite distinct. Table 1 lists the values of KV_m and τ_0 obtained from linear regression. The values obtained for $p = 1$ and $\tau_0 = 10^{-9}$ s are also shown. A considerable discrepancy is observed for both KV_m and τ_0. The value of τ_0 determined from the χ'' peaks, however, is quite close to the correct value.

To estimate in a more general sense the deviation resulting from this incorrect use of T_p, we use the replacement $T_B = (1/\beta)(T_p - \alpha)$ and obtain

$$\ln(\omega) = \ln(1/\tau_0) - \frac{KV_m}{k_B}\frac{\beta}{T_p - \alpha}. \tag{23}$$

While this is not a linear function in $1/T_p$, it closely resembles one when T_p falls within the range of values typically encountered. The slope and intersect, however, are different from KV_m/k_B and $\ln(1/\tau_0)$ as may be shown by a first order Taylor expansion of equation (23) around a point $1/T_0$, suitably chosen in the middle of the range of $1/T_p$ for the dataset. This gives

Table 1. Apparent values of KV_m/k_B and τ_0 (for $\sigma_V = 0.5$) obtained when T_p is taken as T_B in (22). The correct value of KV_m/k_B is 267 K.

τ_0 (s) p	10^{-11} 1/2	10^{-11} 1	10^{-9} 1/2	10^{-9} 1
	$(KV_m)_{\text{apparent}}/k_B$ (K)			
From χ'	346	444	346	445
From χ''	207	266	207	266
	$(\tau_0)_{\text{apparent}}$ (s)			
From χ'	5.8×10^{-12}	5.8×10^{-12}	5.6×10^{-10}	5.6×10^{-10}
From χ''	1.1×10^{-11}	1.1×10^{-11}	1.1×10^{-9}	1.1×10^{-9}

$$\ln(\omega) \approx \ln(1/\tau_0) + \frac{KV_m}{k_B}\frac{\alpha\beta}{(T_0-\alpha)^2} - \frac{KV_m}{k_B}\frac{T_0^2\beta}{(T_0-\alpha)^2}\frac{1}{T_p} \tag{24}$$

from which we obtain

$$\ln(\tau_0)_{\text{apparent}} = \ln(\tau_0) - \frac{KV_m}{k_B}\frac{\alpha\beta}{(T_0-\alpha)^2}, \tag{25}$$

and the slope

$$\left(\frac{KV_m}{k_B}\right)_{\text{apparent}} = \frac{KV_m}{k_B}\frac{T_0^2\beta}{(T_0-\alpha)^2}. \tag{26}$$

This demonstrates why different values of KV_m/k_B and τ_0 are found when T_B is replaced by T_p in equation (22). Note the consequences of having $\alpha \neq 0$. If $\alpha = 0$, the intersect would be unaffected and the slope would simply be modified by the factor β, making the analysis much simpler. As shown here, simply using T_p as T_B will lead to erroneous values of KV_m and τ_0. This is also the case if it is assumed that $T_p = \beta T_B$. Thus, the finite value of α generally cannot be ignored.

From (25) we see that the sign of α determines whether the value of τ_0 is over- or underestimated. From figure 3 we see that for $\sigma_V > 0.2$, $\alpha' > 0$, hence τ_0 will in most cases be underestimated. A detailed analysis (not shown here) has revealed that the relative error in the determination of τ_0 depends mainly on σ_V, whereas it is independent of p and depends only weakly on τ_0. This is also demonstrated by the values listed in table 1. As the present analysis has shown, however, the magnitude of α'' is typically small compared to the peak values. Consequently, the error in the determination of τ_0 will be minimal when peaks of the out-of-phase susceptibility data are used, whereas using the in-phase data will give considerable errors. It is important, however, to keep in mind that this only holds when T_B is defined in terms of the median volume. Had we used instead the average volume, different results would have been obtained, since for a log-normal distribution it is well known that $\langle V\rangle/V_m = \exp(\sigma_V^2/2)$. Consequently, the blocking temperature defined in terms of $\langle V\rangle$ would be larger, giving different values of α', β', α'', β''.

The advantage of using equation (22) to determine τ_0 and KV_m is that one avoids having to do a full-curve fit to expressions like (17) and (18). The analysis presented here, however, shows that, without knowledge of α and β, this approach may yield systematic errors in the estimates of KV_m and τ_0. It should be noted, though, that for $p = 1$, $\alpha'' \approx 0$ and $\beta'' \approx 1$ and is almost independent of σ_V. Thus, for ferromagnetic particles the error in τ_0 and KV_m will be negligible if the χ'' data are used for the analysis. In the case of antiferromagnetic particles, the χ'' data will give almost correct values for τ_0, but not for KV_m. If the χ' data are used in the analysis, the values of τ_0 and KV_m will be incorrect both for ferromagnetic and antiferromagnetic particles. Better estimates of KV_m may, in principle, be obtained by using (25) and (26) and the appropriate values of α and β, which may be obtained if the values of τ_0, p and σ_V are approximately known. However, if the data are not compromised by, e.g., impurity signals, a full-curve analysis may prove rather simple and will yield more accurate values of not only KV_m and τ_0, but also σ_V and p [19]. If the quality of the data does not permit such an analysis, it should be kept in mind, though, that the most accurate results are obtained from the χ'' peak positions.

6. Summary

We have studied the correlation between superparamagnetic blocking temperatures and peak temperatures obtained from ac magnetization measurements. We obtain different results for ferromagnetic materials and antiferromagnetic materials due to the different relation between volume and magnetic moment. If the anisotropy energy barrier KV_m and the attempt time τ_0 are determined directly from the peak positions, these relationships must be taken into consideration. Otherwise, only rough estimates of KV_m and τ_0 may be obtained. Through the analysis presented here we have quantified the error resulting from the uncritical use of the peak positions, and have found that the magnitude of this error depends on the parameters p, τ_0, σ_V. For ferromagnetic particles, though, using the peak positions of χ'' will give rather accurate results. For $p < 1$ the value of τ_0, but not KV_m, may be determined with good accuracy from χ'' peak positions. Furthermore, if one compares peaks temperatures obtained from χ' data with those obtained from χ'', a relationship is found which is independent of the type of (magnetic) material. This may be utilized to determine the width of the particle size distribution.

Acknowledgments

This work was supported by the Danish Research Council for Technology and Production Sciences.

Appendix

In the expressions for χ' and χ'' (12)–(14) it is usually assumed that there is a relationship between the particle volume and the magnetic moment. However, if the magnetic moments are due to randomness of the occupation of lattice sites as in antiferromagnetic nanoparticles, this is not the case. Particles with a given volume, V, can have different moments, described by a distribution function, $\rho_V(\mu_u)$. The contribution to the ac susceptibility from the particles with volume V is then given by

$$\chi_{ac}(\omega, T) = \int_0^\infty \frac{\chi_\infty + i\omega\tau\chi_0}{1 + i\omega\tau} \rho_V(\mu_u)\, d\mu_u. \quad (A.1)$$

Because $M(V) = \mu_u / V$ we find by inserting (10) and (11) in equation (A.1)

$$\chi_{ac}(\omega, T) = \frac{\mu_0}{1 + i\omega\tau}\left[\frac{V}{3k_B T} + \frac{i\omega\tau}{3K}\right] \times \frac{1}{V^2}\int_0^\infty \mu_u^2 \rho_V(\mu_u)\, d\mu_u. \quad (A.2)$$

Thus one obtains the correct expressions for $\chi_{ac}(\omega, T)$ by substituting $M^2(V)$ by the second order moment of the magnetization distribution

$$M^2(V) = V^{-2}\int_0^\infty \mu_u^2 \rho_V(\mu_u)\, d\mu_u \quad (A.3)$$

in (12)–(14).

References

[1] Leslie-Pelecky D L and Rieke R D 1996 *Chem. Mater.* **8** 1770
[2] Dormann J L, Fiorani D and Tronc E 1997 *Adv. Chem. Phys.* **98** 283
[3] Kodama R H 1999 *J. Magn. Magn. Mater.* **200** 359
[4] Batlle X and Labarta A 2002 *J. Phys. D: Appl. Phys.* **35** R15
[5] Fiorani D (ed) 2005 *Surface Effects in Magnetic Nanoparticles* (New York: Springer)
[6] Mørup S, Madsen D E, Frandsen C, Bahl C R H and Hansen M F 2007 *J. Phys.: Condens. Matter* **19** 213202
[7] Madsen D E, Mørup S and Hansen M F 2006 *J. Magn. Magn. Mater.* **305** 95
[8] Silva N J O, Amaral V S and Carlos L D 2005 *Phys. Rev.* B **71** 184408
[9] Néel L 1961 *C.R. Hebd. Seances Acad. Sci.* **252** 4075
[10] Néel L 1962 *Low-Temperature Physics* ed C DeWitt *et al* (New York: Gordon and Breach)
[11] Richardson J T, Yiagas D I, Turk B, Forster K and Twigg M V 1991 *J. Appl. Phys.* **70** 6977
[12] Gittleman J I, Abeles B and Bozowski S 1974 *Phys. Rev.* B **9** 3891
[13] Néel L 1949 *Ann. Geophys.* **5** 99
[14] Brown W F 1963 *Phys. Rev.* **1** 1677
[15] Lundgren L, Svedlindh P and Beckman O 1981 *J. Magn. Magn. Mater.* **25** 33
[16] Lundgren L, Svedlindh P and Beckman O 1982 *Phys. Rev.* B **26** 3990
[17] Jiang J Z and Mørup S 1997 *Nanostruct. Mater.* **9** 375
[18] Hansen M F and Mørup S 1999 *J. Magn. Magn. Mater.* **203** 214
[19] Madsen D E, Hansen M F, Bendix J and Mørup S 2008 *Nanotechnology* **19** 315712